From SSTO to Saturn's Moons: Superperformance Fusion Propulsion for Practical Spaceflight

By Robert W. Bussard and Lorin W. Jameson, Energy/Matter Conversion Corporation, 680 Garcia Street, Santa Fe, NM 87505, <emc2qed@comcast.net>

Abstract

Extremely advanced space propulsion systems can be based on use of inertial electrostatic fusion (IEF) power sources of very light weight and large power density and output, that use $p^{11}B$ or $^3He^3He$ fusion reactions for radiation-free production of very energetic charged particles. These can be used to heat propellant by mixing with diluent, or by direct conversion to electrical power at high voltage to drive relativistic e-beams (reb) for heating. Such engine systems can be applied to the full spectrum of space flight from earth-to-orbit to cis-lunar to near-interstellar travel. Fast transits with high payloads in single-stage vehicles can be achieved to the inner planets (IP) with IEF engines using reb-heated propellant, while comparable performance to the outer planets (OP) and quasi-interstellar (QIS) missions uses magnetic confinement for direct heating of propellant by mixing with IEF fusion products. The IEF engine performance spectrum ranges from thrust-to-mass ratios of $[F] = 6$ at $I_{sp} = 1500$ sec to $[F] = 0.005$ at $I_{sp} = 1E6$ sec. Estimates of costs and time scale for their development and for operating costs for SSTO, Earth/Mars and Earth/Saturn orbital missions show 2-4 orders of magnitude reduction from current solar system transport costs, suggesting that practical space flight could be flight-proven by 2020.

Nomenclature

A_{rad} = waste heat radiator area

a_o = initial vehicle force acceleration

a_f = final vehicle force acceleration

a_{rad} = radiator mass coefficient

F = thrust

$[F]$ = engine system thrust/mass ratio

G_{gross} = ratio gross electric to drive power

I_{sp} = engine system specific impulse

I_s = net effective I_{sp}

$[I_{sp}]$ = normalized $[I_{sp}] = I_{sp}/1000$

m_o, M_o = vehicle gross mass

m_e, M_E = engine system mass

m_p = propellant mass

m_L, M_L = payload mass

P_f = fusion power (MWth)

P_e, P_{net} = electric power (MWe)

P_E = propulsive jet thrust power

t_b = engine thrusting time

t_c = vehicle coasting time

v = vehicle speed

δS = incremental distance traversed

δv_c = "characteristic" velocity of flight

1. Introduction

The achievement of effective space flight requires propulsion systems of large flight-path-averaged specific impulse (I_{sp}) and engine system thrust-to-mass ratio ($F/m_e = [F]$). If $[F]$ is greater than the local gravitational acceleration, then all flights will be "high-thrust" in character, and minimal transit times can be achieved for any vehicle configuration and mass distribution. With such engines, economically-useful payload fractions can be carried over large velocity increments by single-stage vehicles with practical structural factors. For short transit times in most missions it is found that the limited energy available from chemical combustion reactions limits payload fractions to small values, even with multiple-stage vehicles, and single-stage vehicles are not feasible for rapid (e.g. less than one year) interplanetary flights. Greater payload fractions with short flight time

can be achieved *only* with high-I_{sp} engines[1] that also have "high-thrust" capabilities.

But this requires both light weight and a sufficiently energetic propulsion system to drive these vehicles.[2] The inherent high-I_{sp} advantages of most nuclear fission propulsion concepts are compromised[3] by hazardous radiation output requiring massive radiation shielding that negates most of their performance improvements.[4] However, non-radiative nuclear reactions exist that do *not* require massive shielding, and that yield only energetic charged particles for direct thermal or electrical power production.

These include fusion reactions between the fuels p (^{1}H), ^{11}B, and ^{3}He. These can be "burned" in inertial-electrostatic-fusion (IEF) devices[5,6] that use new methods for dynamic confinement of fusion-reactive ions by special magnetic-electric-potential means[7] or by inertial-collisional-compression (ICC)[8] of plasma fuel ions. Such IEF power sources can provide quiet-electric-discharge (QED) direct-converted electrical power[9,10] at high voltage (MeV) to heat and expand or to accelerate directly a working fluid to provide rocket thrust at high specific impulse (I_{sp} from 1500 to 70,000 sec). These QED engine systems are most useful for ground-to-orbit (SSTO) and solar system inner planet (IP) flights.

Alternatively, the charged ionic fusion products can be trapped in a toroidal magnetic field configuration around an IEF fusion source and used to heat directly a propellant/diluent. Such a diluted-fusion-product (DFP) engine system avoids the difficulties and thermal limitations of energy conversion equipment and allows attainment of extremely high I_{sp} - up to that of the fusion products alone (I_{sp} ≈ 1.4E6 sec) as required for long-range outer planet (OP) and QIS missions.

Here, a summary is given of the features and performance ranges of QED fusion direct-electric engine systems and of thermal DFP engine systems at higher I_{sp}. Using this information, several selected example vehicles/spacecraft are defined and a simple analysis is made of their application to three missions:

(a) Single-Stage-To-Orbit (SSTO) flight from ground to a low Earth orbit (LEO) at 300 nautical miles;

(b) Fast transit between the orbits of Earth and Mars, and;

(c) Fast transit from Earth's orbit to the orbit of Saturn.

The vehicle flight performance found for these three missions is used to assess their costs of payload transport, based on various assumptions of the costs of system development, manufacture and use. The range of specific impulse used for these missions varies from about 2300 sec to 70,000 sec.

2. QED Engine Systems

The simplest and most direct engine system is all regeneratively-cooled (ARC) and employs direct-electric-driven quasi-relativistic e-beams (reb) for 100% efficient heating of air or rocket propellant to extreme temperatures, with resulting high specific impulse exhaust performance capabilities.[11] This basic QED rocket engine configuration is shown in schematic outline in Figure 1. The upper limit performance of this ARC/QED engine is set by the maximum limiting cooled-structure temperature.

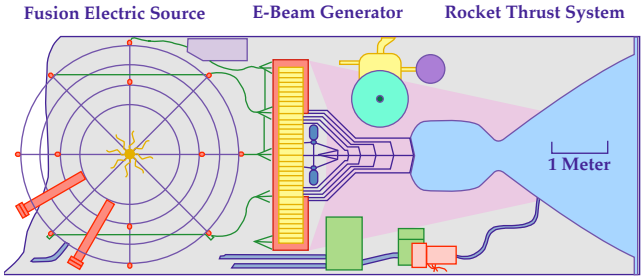

Figure 1 — Schematic outline of ARC/QED engine system

Higher I_{sp} can be attained by use of controlled space radiators (CSR) to handle waste heat loads. However, the upper I_{sp} limit of such thermal (here called CSR-A) systems is, once again, thermal; it is the limiting temperature that can be sustained by nozzle walls. This is set by thermal *radiation* from propellant gas to the walls, which can *not* be inhibited by the convection-insulating nozzle wall *B* fields. Beyond this limit it is necessary to use the IEF-generated direct-electric power to drive still higher exhaust speeds in a *non*-thermal manner, by use of collective acceleration in electron-beam traveling-wave fields. The performance of this (CSR-B) system is set by the absolute limit of unavoidable waste heat cooling. This is about 1E-4 of system total power, due to gamma and X-ray heating of cryogenic structures required for the super-conducting magnets.

These CSR-A,B engine systems scale differently than ARC engines, following more complex scaling algorithms that reflect the variable mass of waste heat radiator required as the system I_{sp} is increased above the ARC limiting values. Figure 2 gives schematic outlines of each of these QED engines, in sequence, showing the principal subsystems of each complete QED engine system, as described above.

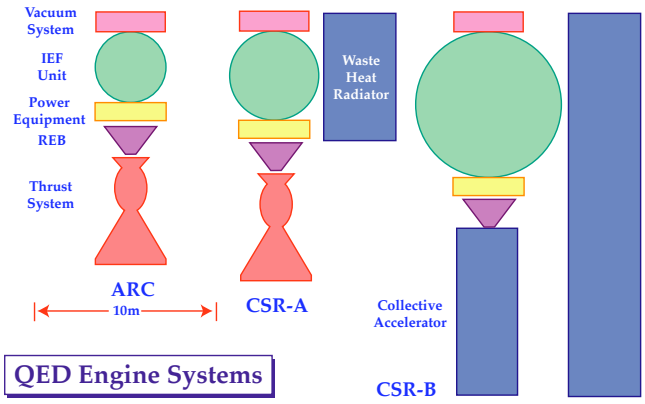

Figure 2 — Schematic outline of sequence of QED engines

The design and performance of these engine systems has been detailed previously,[12] and is given in summary form in Figure 3, which plots propellant exhaust specific impulse I_{sp}, as a function of engine system thrust/mass ratio [F] in comparison with performance projections for other concepts for fusion propulsion.[13] The ARC and CSR engine performance curves shown are based on IEF sources using $p^{11}B$ fusion fuels; these outperform all other advanced concepts for fusion propulsion by 2-3 orders of magnitude. The $^3He^3He$ reaction can not be used practically in the ARC/CSR engine concepts because of the difficulty of direct electric conversion of the wide energy spread of its fusion products (however it could be used in thermal DFP engines for OP/QIS flight missions).

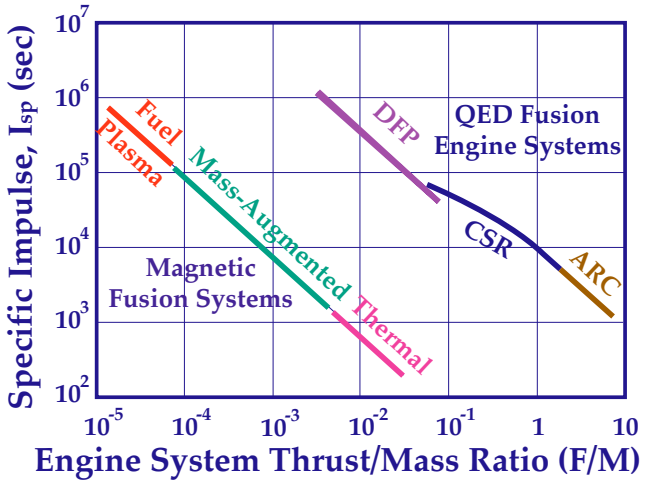

Figure 3 — QED engine performance, showing I_{sp} variation with thrust-to-engine-mass ratio [F] compared with conventional magnetic fusion concepts.[5]

Propulsion system performance beyond even these levels is required for practical space flight to more distant, longer missions such as for fast transits to the outer planets or to the solar-lens gravitational point (550 A.U.), or to further quasi-interstellar distances. For such missions, the usual QED engine thermally limited direct-electric-conversion systems must be abandoned in favor of systems that use direct-fusion product (DFP) propellant heating, without the medium of intervening mass-accelerating machinery. The performance range of such DFP engines using $p^{11}B$ fuel is also shown in the figure. These are discussed in more detail in following sections.

3. IEF Power Sources

The IEF fusion-electric source systems use quasi-spherically-symmetric polyhedral magnetic fields to confine electrons which are injected at high energy E_o, so as to form a negative electric potential well that can confine fusion ions in spherically-converging flow. Figure 4 shows a schematic diagram of this electron acceleration (EXL) IEF system. Fusion ions are inserted into the well near its boundary R, so that they "fall" towards the center and oscillate across the machine, with density increasing rapidly ($1/r^2$) towards the center. Their injection rate is controlled (relative to electron drive current) so that their core energy reaches a specified (required) central virtual anode height $\eta = \delta E_o$. They reach maximum density at a core radius set by the ratio of their initial transverse energy $dE_\perp$ at injection, to their energy $E_c = (1-\eta)E_o$ at the core boundary r_c as given by $< r_c > = r_c/R = (dE_\perp/E_o)^{0.5}$. Typical ion convergence ratios are $0.001 < < r_c > < 0.01$, which yield core densification of 1E4-1E6 above the minimum ion densities in the system.

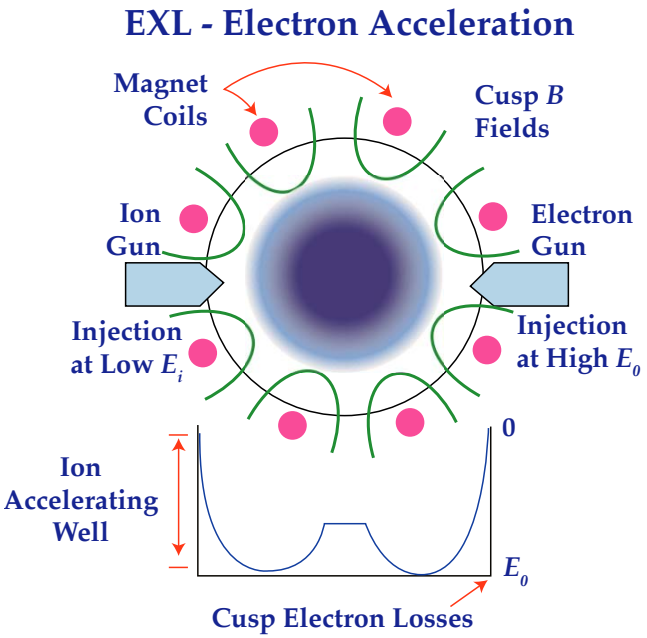

Figure 4 — The EXL/IEF concept; ion acceleration by electron-injection-driven negative potential well maintained in polyhedral magnetic field

Clean Fusion Reactions

Desirable fusion reactions yield only charged particle products. Such reactions have no radiation hazards from energetic neutrons which always characterize fusion in

deuteron-bearing mixtures. Clean fuels for QED and DFP propulsion engine applications are p (^{1}H), ^{11}B, and ^{3}He, reacting according to:

$$p + {}^{11}B \longrightarrow 3\ {}^{4}He \qquad (8.68\ MeV) \qquad (1)$$

$$^{3}He + {}^{3}He \longrightarrow {}^{4}He + 2p \qquad (12.9\ MeV) \qquad (2)$$

Direct production of electric power from these reactions is by deceleration of the charged fusion product ions in an externally-imposed electric field. These move predominantly radially from their central birth point in the IEF core and can be collected, as they approach zero kinetic energy, by grids or plates placed at appropriate radial positions along their path. These collectors are connected to the electrical circuit driving current through the system external load.

In such a direct conversion system (DCS) the easiest fusion products to direct-convert are those of 1, because of the well-defined energies of the fusion product alphas.[19] These are roughly 2.46 MeV and 3.76 MeV and, since their charge is $Z = 2$, electric field deceleration requires a retarding potential of only about 1.9 MeV. This is supplied by spherically symmetric grids located 0.5-1 m outside of the IEF ion-confining region. Thus, direct-conversion $p^{11}B$ IEF systems need be only about 1-2 m larger in diameter than the size required for producing the controlled fusion process, itself.

The second reaction is not suited to direct electrical power production because the energy distribution of the reaction products in 2 is continuous rather than discrete, and the proton energy can range from about 10.7 MeV to nearly zero, with a corresponding variation of alpha energy from 1.1 MeV to 6.4 MeV. Converting the maximum proton energy requires DCS structures of sizable radial dimensions (ca. 5-10 m), and the energy spread forces use of many collection grids. This poses mechanical and thermal problems considerably worse than those for $p^{11}B$. The $^{3}He^{3}He$ system seems suited to propulsion use only through direct heating in a diluent/propellant system-

For extremely high I_{sp}, as needed for high performance in OP/QIS flight, it is impractical to use energy conversion machinery for main power in any event, because even minor inefficiencies pose insuperable thermal loads and waste heat disposal requirements that can be met only with massive space radiator and internal cooling systems and equipment. Again, the $p^{11}B$ cycle yields smaller and simpler engines than does $^{3}He^{3}He$, which is not considered further.

System Configuration Considerations

The EXL system consists of a set of polyhedral magnet coils that confine electrons, which make a negative ion-confining well, as suggested in Figure 4. The whole unit is sealed within a spherical vacuum shell that constitutes the outer conductor of the direct-electric power system. The shell is pumped to maintain the vacuum required for system operation (e.g. < 1E-6 torr), and any unburned fuel is recycled through the vacuum system. The EXL unit output is coupled to power conversion equipment that drives a short e-beam accelerator, whose beam is fed into the rotational-flow rocket thrust chamber. Details and power/mass scaling of this system have been given elsewhere.[14,15,16]

In the DFP engine application the IEF source configuration is very much simpler than for use in QED/ARC/CSR engines. This is precisely because there is no external vacuum shell directly surrounding the EXL fusion system, thus eliminating the need for structure and cooling of such a shell. Here the magnet coils define the active radial boundary (R) of the source, and the fusion products escape the EXL device and heat propellant/diluent by collisions outside the EXL unit, as shown in Figure 5.

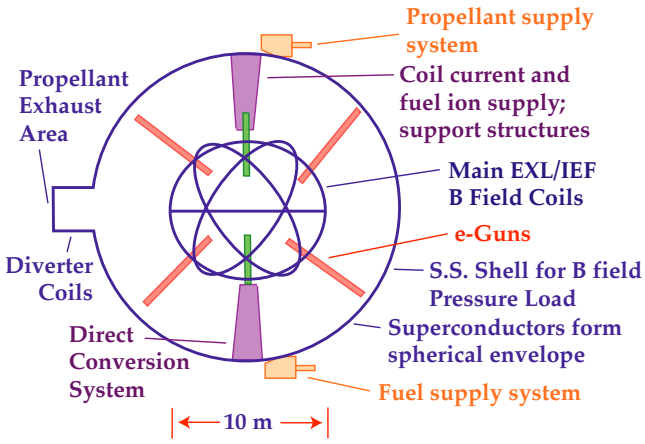

Figure 5 — Schematic outline of DFP engine, showing IEF placement, confinement/thrust shell, and magnetic diverter exhaust "nozzle"; thrust is to right

The fusion products are captured external to the EXL unit by a surrounding magnetic torus of small aspect ratio. They are held long enough to heat (by collision) the diluent that is introduced to reach the desired I_{sp} and thrust conditions. The fusion source is open to the vacuum region of the propellant/diluent mixing region which, itself, is open to space as its main vacuum pumping system. Unburned fusion fuel is prevented from loss by use of special "limiters" placed inside the EXL coil system, that capture escaping fuel ions and recycle them through the fuel supply system. Toroidal magnetic fields needed for proper diluent mixing with fusion products are smaller than those for the EXL unit. The toroidal field is driven by current through the external shell, which serves as the return path for current flow through the entire system. Design considerations for this engine system have been presented in an earlier paper,[17] its performance is as shown in Figure 3, previously.

4. Mission Performance Economics

Using the engine system performance shown in Figure 3 for the three classes of QED/DFP engines discussed above, it is possible to estimate payload transport costs for any defined mission. The three missions chosen for consideration here are the SSTO mission to LEO, an Earth/Mars' orbit transfer, and a fast transit from Earth's orbit to that of Saturn.

SSTO Mission

The SSTO flight was studied using a winged vehicle as shown in Figure 6, with a gross takeoff weight (GTOW) of 250,000 kg. The vehicle was driven to orbit along a specified fly out trajectory, using turbojet propulsion up to Mach 2.5, with rocket propulsion by two QED/ARC engines of about 5300 MWt output thereafter.

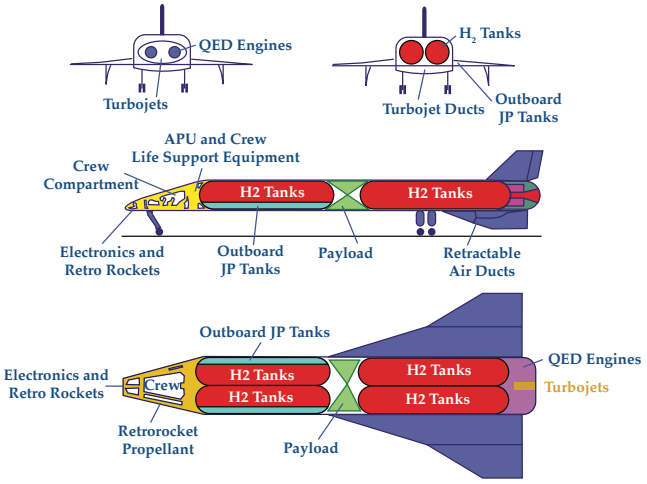

Figure 6 — Schematic outline; QED/ARC SSTO vehicle

The net effective I_{sp} varied with flight speed as given in Figure 7. Results showed that approximately 0.62 of GTOW could be carried to LEO at 300 nautical miles in an equatorial eastward launch.

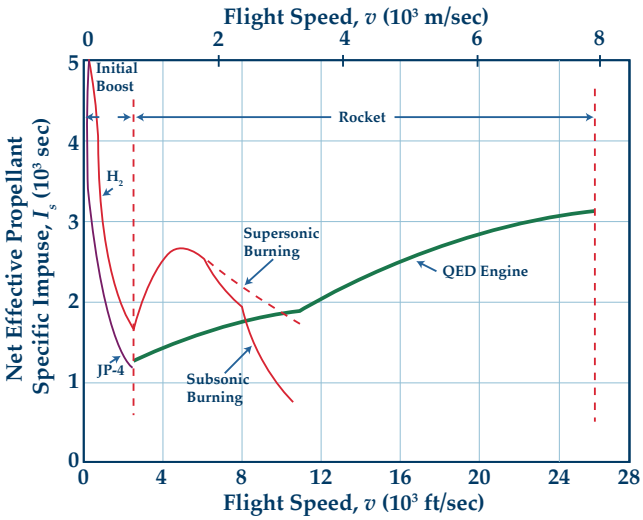

Figure 7 — Net I_{sp} vs. flight speed; SSTO system

Accounting for all structure and subsystem weight (landing gear, empennage, wings, jet engines, crew compartment, et al) with a dry weight fraction of 0.48 gives a payload fraction of 0.14. This is a payload of 35,000 kg delivered to orbit in each flight.

It was assumed that the vehicle manufacturing cost was $1000/kg, giving a single unit cost of $120M. Allowing a life cycle of 240 flights (for example, 24 flights per year over 10 years), the direct capital cost charges are only $ 14.29/kg delivered to LEO. Taking 0.5 of this ($7.14/kg) for maintenance costs adds $2.5M to the cost of each flight. The cost of propellant (H_2O, NH_3, LH_2) assumed at $1.00/kg adds another $2.72/kg for total $24.15/kg cost of payload to LEO.

To account for system R&D, assume that development requires $10B for the complete engine plus vehicle operational system, and that this is allocated over 100,000 vehicle-flights. This is equivalent to 200 flights (life cycle) for each of 50 vehicles, and very much less than the ca. 2E7 vehicle flights per year of the world aircraft industry. This adds about $100K per vehicle flight. Finally, allow profit generation at 100% of the direct cost of capital and operations (above). The cost additions then become $2.86/kg and another $24.15/kg, respectively.

Under these assumptions the total price for payload delivery to the chosen orbit is still only $51.16/kg, about 1/200 of current rocket vehicle costs to orbit. About 47% of this is profit at a net rate of return of about 16.9% on the $120M capital cost of the vehicle. In contrast, if the system were government owned, with no profit/ROI , the delivery costs would be only $27.01/kg ($12.28/lb) to LEO. This great reduction in cost from current practice results from the very high performance of the engine/vehicle system; about 20 times greater payload delivery per unit mass of vehicle than for the Shuttle system. The sine qua non for such a system is the QED/ARC fusion engine.

It is estimated that this can be developed for about 20% of the total system R&D cost, above, and that testing of the engine concept could be accomplished for about $500-700 M over a 6-8 year time frame. If this early work showed clear proof-of-feasibility, first flight system applications should be possible with 7-9 years additional R&D, thus giving a practical means of access to space by 2020 or so.

Earth/Mars (E/M) Transfer

A second mission of interest was the transfer of payload from Earth's orbit to the orbit of Mars; recognizing that velocity matching and capture at either end of this flight could require velocity increment capability larger than that for the transit itself. However, proper orbit mechanics can be used to assist matching and capture to the moons of either planetary body, and the large hyperbolic excess velocity used in the analysis tends to overwhelm these second order requirements. All vehicles studied were limited to single-stages, to avoid the complexities, costs and inherent non-reusability of multiple-staging.

Study of the use of QED engines for E/M flights showed that there was a minimum power output that characterized efficient engines. Below this power the engine mass decreased only slowly, thus there is no incentive to seek vehicles that require less power.

Table 1 — Earth/Mars Orbit Transfer Space Vehicle Performance With Minimum QED Engine Systems

Performance Parameter	ARC System	CSR-A System
m_o, Gross mass	500T	500T
m_L, Payload	72T	103T
m_p, Propellant	360T	335T
m_L, Engine system	20T	16T
A_{rad}, Radiator	0	3.0E3 m²
P_L, Thrust power	6.0 GW	1.0 GW [*2]
I_{spo}, Initial I_{sp}	5500 sec	5500 sec
I_{spf}, Final I_{sp}	5500 sec	7800 sec
F_o, Engine	22.5T	1.88T
F_f, Thrust	22.5T	1.33T
a_o, Engine force	45.0 mg_o	3.76 mg_o
a_f, acceleration	159.0 mg_o	8.06 mg_o
δv_c, Max delta-v	67.4 km/s	71.0 km/s
t_{b1}, Burn 1 time	0.74 day	9.3 day
δS_1, Distance	1.0 Mkm	13.4 Mkm
t_{c12}, Coast time	32.3 day	123.3 day
δS_{12}, Distance	90.1 Mkm	68.4 Mkm
t_{b2}, Burn 2 time	0.24 day	6.3 day
δS_2, Distance	0.3 Mkm	9.6 Mkm
t_{total}, Total flight time	33.2 day	37.9 day
δS_{total}, Total distance	91.4 Mkm	56.8 Mmile

*[*2] CSR thrust systems; 1 on, 1 off; 1 rad.*

It was found from this that ARC and CSR-A systems could be used effectively at all vehicle sizes above about 500,000 kg gross full weight (mass), but that smaller systems made progressively less use of the minimum QED engine. Vehicles up to 10,000 metric tonnes (T) were analyzed, using both types of QED engine system.

The results showed that the minimum 500 T system could deliver over 20% payload with a single-stage vehicle, with a total transit time of less than 38 days, using an acceleration/coast/deceleration trajectory. Such fast E/M transfers could be made over about 1/3 of each year. The other 2/3 of the time would require somewhat longer transits; up to 60-70 days for another 1/3 of the year. Table 1 summarizes the results for both CSR-A and ARC engines. Note that the maximum speed (67-73 km/sec) is large compared to capture delta-v needs, thus these can affect the transit times estimated here by, at most, 10-15%.

From this information it is possible to estimate payload transport costs, on the assumption that the vehicle can be refilled with propellant at each end of each one-way journey. Since water can be used as a propellant/diluent, this should be quite simple at Mars as well as Earth. Fusion fuel supply is of little consequence, being only a few hundreds of kilograms, at most, for each round-trip flight.

To assess economic prospects, assume that the CSR-A vehicle is used. This bas a 3000 m² waste heat radiator whose mass (of 1000 kg) is included in the total QED engine system mass of 16.0 T. It operates at a relatively low force acceleration but with variable high I_{sp} to optimize flight. Because of this it delivers about 43% more payload (103 T vs. 72 T), albeit with 4.7 days longer flight time, than does the ARC engine-powered vehicle. Both systems use "1/e" vehicles in which 0.632 of the gross vehicle mass is taken for propellant. This semi-optimizes IP flight so that the total characteristic velocity capability of such systems is always $\delta v_c = g_o I_s$, where I_s is the flight averaged specific impulse.

System costs are estimated by taking manufacturing cost as $1500/kg for all structure and systems excluding the engine system, which is costed at $5000/kg. The vehicle has 103.0 T of payload (including crew, electronics, etc) capability, with 65.0 T of basic structure and 16.0 T of QED/CSR-A engine system (including 1.0 T of radiator). Using these masses gives the total vehicle cost as $177.5 M. If an additional mass charge of 25.0 T is taken from the payload for crew, life support, communications, auxiliary systems, etc, and this is costed at $2500/kg, the total operational system cost becomes $240M, with a net load transport capacity of 78.0 T per one-way (OW) flight, or 156.0 T for each round trip (RT).

Then allow 100 round trip (RT) flights per vehicle as representative of total system lifetime before replacement. Take 6 round trips per year for these systems (for the CSR-A system this means that the vehicle is in flight about 62% of the time) and deprecate their cost over this life. In addition to this allow a charge of 2% of total vehicle cost for operational maintenance for each flight. And, to account for propellant costs assume that these are simply the (non-profit) delivery cost to LEO, as estimated above for the QED/ARC SSTO system. Finally, allow 10.0% per annum for cost-of-money (i.e. interest charges on vehicle investment, if borrowed capital; or return-on-investment, if fully-funded privately).

Taking all of these factors into account the cost per flight becomes $28.3M. With this, RT payload transport cost for the CSR-A system (with reduced payload fraction; 0.156) is found to be $181.4/kg. Since this is distributed as $109.6/kg for propellant (in LEO), $46.2/kg for O&M and depreciation charges, and only $25.6/kg for interest (cost-of-money), it is clear that lower cost of propellant (e.g. water) supply could best improve the E/M transport system. In a future space-based economy this may be possible by use of lunar resources, whose delivery cost to CSR-A vehicle-accessible orbits could be much reduced from that for supply from Earth. But, even at these levels, the cost of EIM transfer of payload is less than 1 % of *current* costs for payload delivery to LEO.

Fast Transits; Earth to Saturn (E/S)

Assessment of the economic potential for a more demanding flight mission was made by considering a system suitable for fast transits to and from the orbit of Saturn. Here, as before, the velocity increment requirements for matching and capture at the target planets (Earth and Saturn) were ignored as being small relative to the total velocity capability of the vehicles being considered. The error thus introduced is about 5-8% in transit time for these E/S missions.

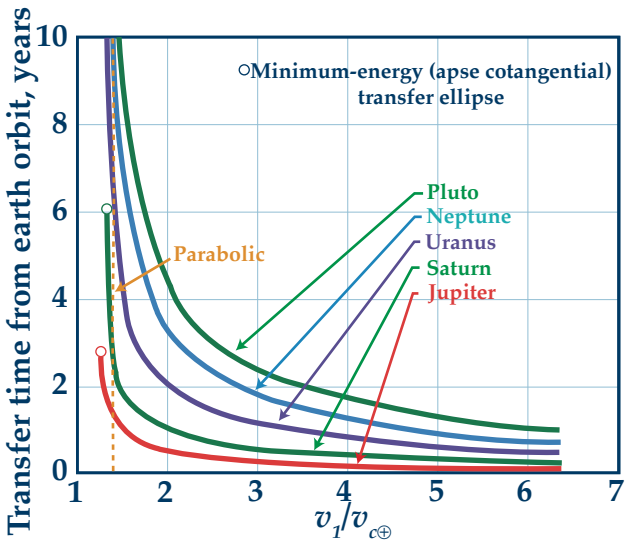

Figure 8 — Earth/OP transit time for hypervelocity flights

The advantage of hypervelocity flight is shown in Figure 8, that gives flight time to the outer planets as a function of the ratio of vehicle burnout speed to Earth's orbital speed in the solar field.[18] The baseline system chosen here has a value of about 11.5 for this velocity ratio. At

this condition, flights with such excess velocity capability follow nearly straight-line Newtonian paths.

Analysis of the size and performance of EXL-based DFP engines gives a reasonable baseline system using a 10,000 MWfus EXL source, running on fusion of $p^{11}B$, in which only about 2% of the fusion products are converted to electricity; only enough to drive the fusion system, itself. Most of the energy is used directly to heat (by collisions) the propellant/diluent injected into the DFP magnetic toroidal thrust system around the EXL source.

This conversion cycle plus that for system cryogeny requires a waste heat space radiator area (one-sided) of about A_{rad} = 2030 m^2; split into two 20 x 100 m units mounted on either side of the engine. Other components include engine thrust shell, shell and IEF coil superconductors, fuel and diluent supply systems, DCS, e-guns, et al. A detailed breakdown of the total mass of this DFP engine system is given in an earlier analysis.[19] From this, the total DFP engine mass is found to be 51,705 kg. It can be operated over an I_{sp} range from about 70,000 sec to 1,000,000 sec or so.

Here, optimum performance for the E/S mission is found at the lower end of the I_{sp} range; the upper range is best used for very deep-space QIS missions (e.g. to the Oort cloud at 550 AU.). While the QED/CSR-B engine can, in principle, also work at this I_{sp} level, it is a much more complex system and more 'highly stressed than is the DFP engine. Here, flight is assumed with I_{sp} = 70,000 sec. Again taking lie vehicles, a baseline vehicle is found at a gross mass of 400,000 kg, of which 252,800 kg is propellant/diluent plus fusion fuel., Tankage and associated structure (exclusive of the engine system) is taken as 25,280 kg (10% of consumables). At the chosen I_{sp} and power level the fusion fuel consumption is about 40.82 gm/sec, over a total thrusting time of 6.154E6 sec, 0.1965 year or 71.7 days. The total mass of fuel is about 900 kg, leaving 251,900 kg for propellant/diluent to be supplied at each end of the E/S journey. Using water as diluent, a spherical propellant tank is found to be only about 3.9 m in radius.

Assuming a crew complement of 12, habitat and operational system space was taken to be 1264 m^3 split between crew quarters, common space, control room, and support services (hospital, library, recreation and exercise rooms, etc.). This was laid out to occupy a cylindrical shell of 7 m outer radius around a hollow central 4 m radius core, in which the payload could be transported in atmospheric conditions. The length of this habitat system is found to be 16.1 m, with a total mass of 25,215 kg, including life support and recycling systems. The remaining mass is available for payload; it is 45,000 kg for each OW flight, or 0.1125 of vehicle gross mass at launch.

The complete vehicle system consists of the 20 m diameter DFP engine, with two 20 x 100 m radiator "wings" parallel to the flight path and extending outwards from the engine, located behind the 4 m radius water/diluent tank inside the aft end of the central core within the 7 m radius x 16.1 m long habitat volume.

With the masses and performance parameters assumed above it is possible to determine flight economics in the fashion used for the E/M flight mission, above. Here, the engine system is casted at $5000/kg;, as before, but costs are allocated to structure at $1000/kg and to habitat at $2000/kg, while propellant on-board is taken to cost $30/kg. For this longer mission, 3 RT flights per year are allowed, depreciation and O&M costs are taken over 100 RT flights/vehicle and at 0.02, and payload is carried in both directions, as before. However, the cost-of-money is chosen to be 9.0% per annum while 16.0% return-an-investment (ROI; profit) is allowed as well.

Using these parameters, the vehicle cost is found to be $334.2 M. If operated without financial charges, the total cost per RT flight is found to be $22.6 M, for a unit cost of $280/kg payload delivered. With these charges included the cost per flight rises to $53.1 M and the unit cost becomes $589/kg, but each flight then makes a RT profit of $17.83M for its owners, or $53.5M/year (from RT flights) per vehicle.

Finally, if R&D costs of $10B are assumed, this represents a return of only 0.535%/year from each vehicle. If 40 vehicles. were constructed and flown, giving 120 round-trip flights per year, the return on R&D would become a respectable 21.4%/year. This would cost $13.4B in new vehicle investment and would involve the transport of 10,800 T/year; about 1 % of the current traffic handled by the world's aircraft transport systems each day.

When launched the initial acceleration is 7.0 cm/sec^2 rising to a final value of 11.55 cm/sec^2 over the "burn" time for this acceleration of 44.63 days. At this time it has reached a free space speed of 343.2 km/sec = 72.1 A.U./year (about 5.07 days/A.U.), while traversing a distance of 4.41 A.U. During this time it will have consumed 157,388 kg of the propellant. The second (deceleration) thrusting period reduces the speed again to zero (in the free space frame), and requires about 27.1 days. Here the vehicle starts with the prior acceleration and rises to 19.03 cm/sec^2, traversing another 2.67 A.U. Propellant consumption is only 95,412 kg during deceleration.

Since the orbit of Saturn lies between 9.0 and 10.0 A.U. from the Sun, the shortest transits from Earth require traversing a distance of at least 8.0-9.0 A.U. As this is greater than the 7.08 A.U. distance traveled during acceleration/deceleration flight of the DFP system, it is necessary to use a coasting period between these two

powered phases of flight. Note that this is not the case for flight to Jupiter, since the minimum E/J distance is 3.0-4.5 A.U. In fact, lower I_{sp} and higher thrust give more optimum E/J flight performance.

5. Conclusions

EXL/IEF dean fusion power sources offer prospects for development of superperformance rocket engines of two differing but related types; the QED and DFP engine systems. The first of these promises practical economic flight for SSTO to IP missions, while the latter offers startlingly low cost economics potential for OP (and more distant) missions. Taken together, these engines seem able to yield space vehicles that can deliver payloads at costs that are two to four orders of magnitude less than by any current means.

In addition, no matter the economics, whether profit or non-profit, these systems are able to make very fast transits with high payloads and in single-stage vehicles. These short flight times offer the first practical hope for means to open up the solar system, both inner and outer planets, to exploration and habitation by humans. It is only by reasonable journeys at affordable costs that any exploration can lead to colonization.

Neither Brendan the Navigator, Leif Ericcson or Columbus populated the New World; the development and rise of low-cost and reliable wind-driven ships of reasonable capacity and ocean-going capability led to colonization of the Americas. Without these sailing ships of ever-growing speed and reliability, and ever-decreasing costs per unit payload, development of the United States would have proceeded much more slowly and probably along quite different lines. Let us proceed with Space, now.

Publishing History

Reformatted and color illustrations added in August 2007 by Mark Duncan. References updated in April 2009.

References

[1] Maxwell Hunter; "Solar System Spaceships," *Thrust Into Space*, Holt, Rhinehart & Winston, NY, 1966, Chapter 5.

[2] Robert W. Bussard and Richard D. DeLauer; *Nuclear Rocket Propulsion*, McGraw-Hill Book Co., NY, 1958.

[3] Robert W. Bussard and Richard D. DeLauer; *Fundamentals of Nuclear Flight*, McGraw-Hill Book Co., NY, 1965.

[4] Robert W. Bussard; "ASPEN-II: Two-Staging and Radiation Shielding Effects On ASPEN Vehicle Performance," LA-2680, June 25, 1962, declassified with deletions September 6, 1967; and in "ASPEN: Nuclear Propulsion for Earth-to-Orbit Aerospace Plane Vehicles," Robert W. Bussard, Proceedings International Conference on Spaceflight, Rome, June 1971.

[5] Robert W. Bussard; "Some Physics Considerations of Magnetic-Inertial-Electrostatic Confinement - A New Concept for Spherical Converging-Flow Fusion," Fusion Technology, Volume 19, March 1991, p.273

[6] Nicholas A. Krall; "The Polywell: A Spherically-Convergent Ion Focus Concept," Fusion Technology., Volume 22, August 1992, p. 42

[7] Robert W. Bussard; "Method and Apparatus For Controlling Charged Particles," U.S. Patent Number 4,826,626, May 2, 1989, assigned to Energy/Matter Conversion Corp. (EMC2).

[8] Robert W. Bussard; "Method and Apparatus for Creating and Controlling Nuclear Fusion Reactions," U.S. Patent Number. 5,160,695; November 3, 1992, assigned to QED, Inc.

[9] Ralph W. Moir and William L. Barr; "'Venetian Blind' Direct Energy Convertor for Fusion Reactors," Nuclear Fusion, Volume 13, 1973, p.35

[10] William L. Barr and Ralph W. Moir; "Test Results on Plasma Direct Convertors," Nuclear Technology and Fusion, Volume 3, 1983, p.98

[11] Robert W. Bussard; "The QED Engine System: Direct Electric Fusion-Powered Rocket Propulsion Systems," Paper #263, Proceedings of the Tenth Symposium on Space Nuclear Power and Propulsion, Albuquerque, NM, 10-14 January 1993.

[12] Robert W. Bussard and Lorin W. Jameson; "The QED Engine Spectrum: Fusion-Electric Propulsion for Air-Breathing to Interstellar Flight," Paper #AIAA 93-2006, 29th Joint Propulsion Conference, Monterey, CA, 28-30 June 1993.

[13] John F. Santarius, "Magnetic Fusion Energy and Space Development," Proceedings of the 24th Intersociety Energy Conversion Conference, IEEE, Volume 5, p. 2525 (1989).

[14] op cit ref. 11

[15] op cit ref. 12

[16] Robert W. Bussard and Lorin W. Jameson; "Design Considerations for Clean QED Fusion Propulsion Systems," Proceedings of the 11th Symposium on Space Nuclear Power and Propulsion, Albuquerque, NM, 9-13 January 1994.

[17] Robert W. Bussard, Lorin W. Jameson and H.D. Froning, Jr.; "The QED Engine: Fusion-Electric Propulsion for Cis-Oort/Quasi-Interstellar (QIS) Flight," Proceedings of the 44th Congress of the International. Astronautical Federation, 16- 22 October 1993, Graz, Austria.

[18] Krafft A. Ehricke; "Interplanetary Operations," Chapter 8 in *Space Technology*, edited by Howard S. Seifert, John Wiley & Sons, NY, 1959, Figure 8-58.

[19] op cit ref. 17, Table 1.